Clim Dyn (2015) 45:1451–1470
DOI 10.1007/s00382-014-2393-0

Effect of wind forcing on the meridional heat transport in a coupled climate model: equilibrium response

Haijun Yang · Haijin Dai

Received: 27 May 2014 / Accepted: 27 October 2014 / Published online: 12 November 2014

Abstract The effect of the ocean surface winds on the meridional heat transports is studied in a coupled model. Shutting down the global surface winds causes significant reductions in both wind-driven and thermohaline ocean circulations, resulting in a remarkable decrease in the poleward oceanic heat transport (OHT). The sea surface temperature responds with significant warming in the equator and cooling off the equator, causing an enhancement and equatorward shift in the Hadley cell. This increases the poleward atmospheric heat transport (AHT), which in turn compensates the decrease in the OHT. This compensation implies a fundamental constraint in changes of ocean–atmosphere energy transports. Several other compensation changes are also identified. For the OHT components, the changes in the Eulerian mean and bolus OHT are compensated with each other in the Southern Ocean, since a stronger wind driven Ekman transport is associated with a stronger meridional density gradient (stronger bolus circulation) and vice versa. For the AHT components, the changes in the dry static energy (DSE) and latent energy transports are compensated within the tropics (30°N/S), because a stronger Hadley cell causes a stronger equatorward convergence of moisture. In the extratropics, the changes in the mean and eddy DSE transports show perfect compensation, as a result of the equatorward shift of the Ferrell Cell and enhancement of atmospheric baroclinicity in mid-high latitudes, particularly over the North Atlantic. This work also shows how the Earth's climate is trying to maintain the balance between two hemispheres: the ocean in the Northern Hemisphere is colder than that in the Southern Hemisphere due to much reduced northward heat transports cross the Equator in the Atlantic, therefore, the atmosphere responds to the ocean with temperature colder in the Southern Hemisphere than in the Northern Hemisphere by transporting more heat northward cross the equator over the Pacific, in association with a southward shift of the intertropical convergence zone.

Keywords Coupled climate model · Atmospheric heat transport · Oceanic heat transport · Hadley cell · Atlantic meridional overturning circulation · Bjerknes compensation

H. Yang (✉) · H. Dai
Laboratory for Climate and Ocean-Atmosphere Studies (LaCOAS) and Department of Atmospheric and Oceanic Sciences, School of Physics, Peking University, 209 Chengfu Road, Beijing 100871, China
e-mail: hjyang@pku.edu.cn

1 Introduction

Assessing the meridional heat transport (MHT) and its oceanic and atmospheric partition is a classical question of the climate research (Carissimo et al. 1985; Vallis and Farneti 2009). As early as in 1970s, Vonder Haar and Oort (1973) have estimated the MHT using the satellite observation of radiative fluxes. One robust feature of the total MHT is that the Earth system is maintained by a hemispherically antisymmetric poleward heat transport with a peak value of about 5.5 PW (1 PW = 10^{15} W) at 35°N/S (e.g., Trenberth and Caron 2001). Another robust picture of the MHT is that the atmospheric heat transport (AHT) dominates poleward of about 30°N/S while the oceanic heat transport (OHT) dominates in the deep tropic (Held 2001; Wunsch 2005; Czaja and Marshall). However, there is a highly debatable question on the relationship between the changes in the AHT and OHT. Bjerknes (1964) first suggested that if the top of atmosphere (TOA) fluxes and the oceanic heat storage did not vary too much, the total energy

transport in the climate system would not vary too much either. This implies that any large variations of oceanic and atmospheric energy transports should be equal and opposite. This simple scenario has become known as Bjerknes compensation (BC). It would be a critical constraint that might reduce the degree of freedom or uncertainty of the climate system. Previous studies have shown the BC is highly dependent on the timescale, latitudes as well as the models (Shaffrey and Sutton 2006; Vellinga and Wu 2008; Farneti and Vallis 2013).

The relationship between the changes in the AHT and OHT has been studied broadly. It has been examined in the frame of internal climate variability (Shaffrey and Sutton 2006; Swaluw et al. 2007; Farneti and Vallis 2013), or under significant external forcings (Zhang and Delworth 2005; Cheng et al. 2007; Vellinga and Wu 2008; Laurian et al. 2009; Drijfhout 2010; Zhang et al. 2010). Both scenarios show the robust feature of the BC in the changes of MHT. However, the compensation "structure" and mechanisms in these two scenarios are radically different. The former (latter) suggests that the BC is valid in the high (low) latitudes. Even in the latter scenario, although the responses of the atmosphere and ocean circulations as well as their thermal structures are more or less the same in the water hosing experiments of different models, the compensation structures are also different among differ models. For example, in Vellinga and Wu (2008) (VW08) the compensation is very efficient at low latitudes and near complete at the equator, but is incomplete farther north across the northern midlatitude storm tracks. The maximum AHT change occurs right on the equator while the maximum OHT change occurs near the 20°N. In Zhang and Delworth (2005) (ZD05) the compensation situation is similar to that in VW08, but the maximum AHT change occurs around 15°–20°N. The overcompensation of AHT to OHT is insignificant in VW08 and ZD05, but significant in Zhang et al. (2010) due to strong cloud feedback in the tropics. In Cheng et al. (2007) (CBC07) the compensation is quite good from the low latitudes to 40°N. The maximum changes in AHT and OHT occur around 20°–30°N. Instead of overcompensation, there is a weak (strong) undercompensation in the tropics (poleward of 40°N).

These modelling studies suggest that the BC remains an open question because of the fundamental controversies on its applicability. The most serious problem is that currently the BC has not been validated from the observations. Even the data are available, the direct calculation of ocean and atmosphere heat transports from velocity and temperature fields would contain big errors, which might be even bigger than the absolute values of AHT and OHT (Wunsch 2005) and may result in practical infeasible to validate the BC in the real world. However, the relationship between changes of the AHT and OHT is deserved to explore extensively and thoroughly, because it might suggest some fundamental mechanisms in maintaining the stability of the Earth's climate. Furthermore, it could help to understand the so-called reversibility of climate change after sudden big natural disasters or anthropogenic forcing.

A coupled climate model is used in this work to study the BC. Different from previous studies, this work investigates the wind effect on the changes of the MHT. A series of wind perturbation experiments are performed to examine how the wind change affects the wind-driven and thermohaline circulations and thus the OHT; and how the oceanic changes in turn affect the atmosphere circulation and the AHT. In the coupled model system, all heat transport components in the atmosphere and ocean are calculated directly from the velocity and temperature (Yang et al. 2014a). This work focuses on the equilibrium response. The transient changes in the MHT will be studied in our next work.

It is found that changes in AHT and OHT compensate very well in the mid-low latitudes when altering the ocean surface wind stress. This is different from previous studies, in which the BC is valid only in either the tropics (Vellinga and Wu 2008) or the high latitudes Atlantic (Shaffrey and Sutton 2006; Swaluw et al. 2007). In the wind experiments, the TOA flux remains nearly unchanged. Both the wind-driven and thermohaline circulations are weakened rapidly in response to the change in surface winds. The tropical (extratropical) oceans are warmed (cooled) due to the slowdown of poleward OHT. The atmospheric Hadley cell (HC) is thus enhanced and transports more heat poleward, compensating the decreased OHT. The good compensation in the tropic should be attributed to the cloud feedback, which affects the shortwave (SW) and longwave (LW) radiation at the TOA oppositely. Several other compensation changes are also identified in this work. For example, for the OHT components, the changes in the Eulerian mean and Bolus OHT are compensated with each other in the Southern Ocean. For the AHT components, the changes in the dry static energy (DSE) and latent energy transports are compensated within the tropics (30°N/S). In the extratropics, the changes in the mean and eddy DSE transports show a perfect compensation. An very important finding is that this work shows how the Earth's climate is trying to maintain the balance between two hemispheres: the ocean in the Northern Hemisphere (NH) is colder than that in the Southern Hemisphere (SH) due to the much reduced northward heat transport cross the Equator in the *Atlantic*, therefore, the atmosphere responds to the ocean with colder temperature in the SH than in the NH by transporting more heat northward cross the equator over the *Pacific*, in association with southward shift of the intertropical convergence zone (ITCZ). This is also identified in a recent work by Marshall et al. (2013).

This paper is arranged as follows. The second section introduces the coupled model and experiments. The third section discusses the spin-up process of the model climate. The fourth section examines the equilibrium response in the mean meridional overturning circulations in both the atmosphere and ocean, and quantifies the different components in the MHT and their changes. The fifth section summarizes the compensation processes. The last section is the conclusion and discussion.

2 Model and experiments

The model used in this study is the Community Earth System Model (CESM, version 1.0) of the National Center for Atmospheric Research (NCAR). CESM is a fully coupled global climate model that provides state-of-the-art simulations of the Earth's past, present, and future climate states (http://www2.cesm.ucar.edu/). CESM1.0 consists of five components and one coupler: the Community Atmosphere Model (Neale et al. 2013), the Community Land Model (CLM4, Lawrence et al. 2012), the Community Ice CodE (CICE4, Hunke and Lipscomb 2008), the Parallel Ocean Program (POP2, Smith et al. 2010), the Community Ice Sheet Model (Glimmer-CISM) and CESM Coupler (CPL7). CESM1.0 has been widely used and validated by the community aerosols(http://journals.ametsoc.org/page/CCSM4/CESM1).

The model grid employed in this study is T31_gx3v7. The atmospheric component CAM5 has 26 vertical levels, with the finite volume nominal 3.75° × 3.75° in the horizontal. The CAM5 is essentially a new atmospheric model with more realistic formulations of radiation, boundary layer, and aerosols (Neale et al. 2013; Meehl et al. 2013). The General features of the model formulation are given by Neale et al. (2010, 2013). The CLM4 has the same horizontal resolution as CAM5. The ocean POP2 uses the grid gx3v7, which has 60 vertical levels. The horizontal grid has a uniform 3.6° spacing in the zonal direction and non-uniform spacing in the meridional direction. It is 0.6° near the equator, extending to the maximum 3.4° poleward of 35°N/S and then decreasing towards higher latitudes. The model physics is described in details in Danabasoglu et al. (2012). The sea ice component CICE4 has the same horizontal grid as POP2. No flux adjustments are used in CESM1.0.

In the CESM POP2, the physical transport terms are partitioned into resolved and unresolved components. The resolved component, such like Eulerian mean mass and heat transport, can be easily obtained using model output temperature and Eulerian mean velocities. The unresolved components, which results from meso-scale and submeso-scale processes, are parameterized using well-recognized schemes. The meso-scale eddy transport is parameterized according to Gent and McWilliams (1990). The eddy-induced advection coefficient varies in space and time (Danabasoglu and Marshall 2007). A variable coefficient provides a better representation of changes in eddy activity resulting from variable surface momentum forcing than a constant value (Long et al. 2013), allowing the model to more realistically capture the circulation response to changing winds, particularly in the Southern Ocean (Farneti and Gent 2011). Submeso-scale eddies is parameterized by the FFH scheme (Fox-Kemper et al. 2008, 2011), depicting the restratifying effect on the mixed layer.

Experiment analyzed in this paper includes a 2,000-year control run (CTRL) and three 500-year wind perturbation runs. The CTRL starts from the rest with standard configurations (http://www.cesm.ucar.edu/experiments/cesm1.0/). The model climate as a whole reaches quasi-equilibrium after a 1,000-year integration (Yang et al. 2014a). In the wind perturbation runs, the sea surface wind stress in the ocean model is artificially reduced to one-tenth (0.1 W), one-third (0.3 W) and one-half (0.5 W) of its counterpart in the CTRL, respectively. The wind forcing to the ice model remains same as in the CTRL. The winds in the atmosphere model do not change artificially, but tend to change in response to the SST change, while the latter is mainly caused by the changes in the oceanic circulation. The wind experiments are parallel to the CTRL during year 1501–2000, and reach quasi-equilibrium after a 500-year integration (Fig. 1). The monthly outputs are used for analysis. The climate changes in the wind runs are obtained by subtracting the corresponding climate in the CTRL. In this paper we focus on the equilibrium responses, except otherwise mentioned, the changes we analysed in this work are averaged over the last 200-year integration.

3 Transient responses in global climate

It is seen that the transient response time scale of the global overall climate to the weakening of the surface wind is around 50 years (Fig. 1). Thereafter the atmosphere appears to reach the equilibrium while the ocean temperature and salinity fields evolve slowly and linearly, reaching the quasi-equilibrium in about 500 years. The global upper ocean (0–1,000 m) becomes colder and fresher while the lower ocean (below 1,000 m) becomes warmer slightly (Fig. 1a, b). The equilibrium responses of the global mean surface ocean temperature and salinity are about −1.8 °C and −1.1 psu in 0.1 W run (−1.3 °C and −0.6 psu in 0.3 W run, −0.8 °C and −0.3 psu in 0.5 W run, figures not shown). The colder global climate in the reduced wind experiments results from the less SW radiation received by the Earth (Fig. 1c), with significant cooling occurring

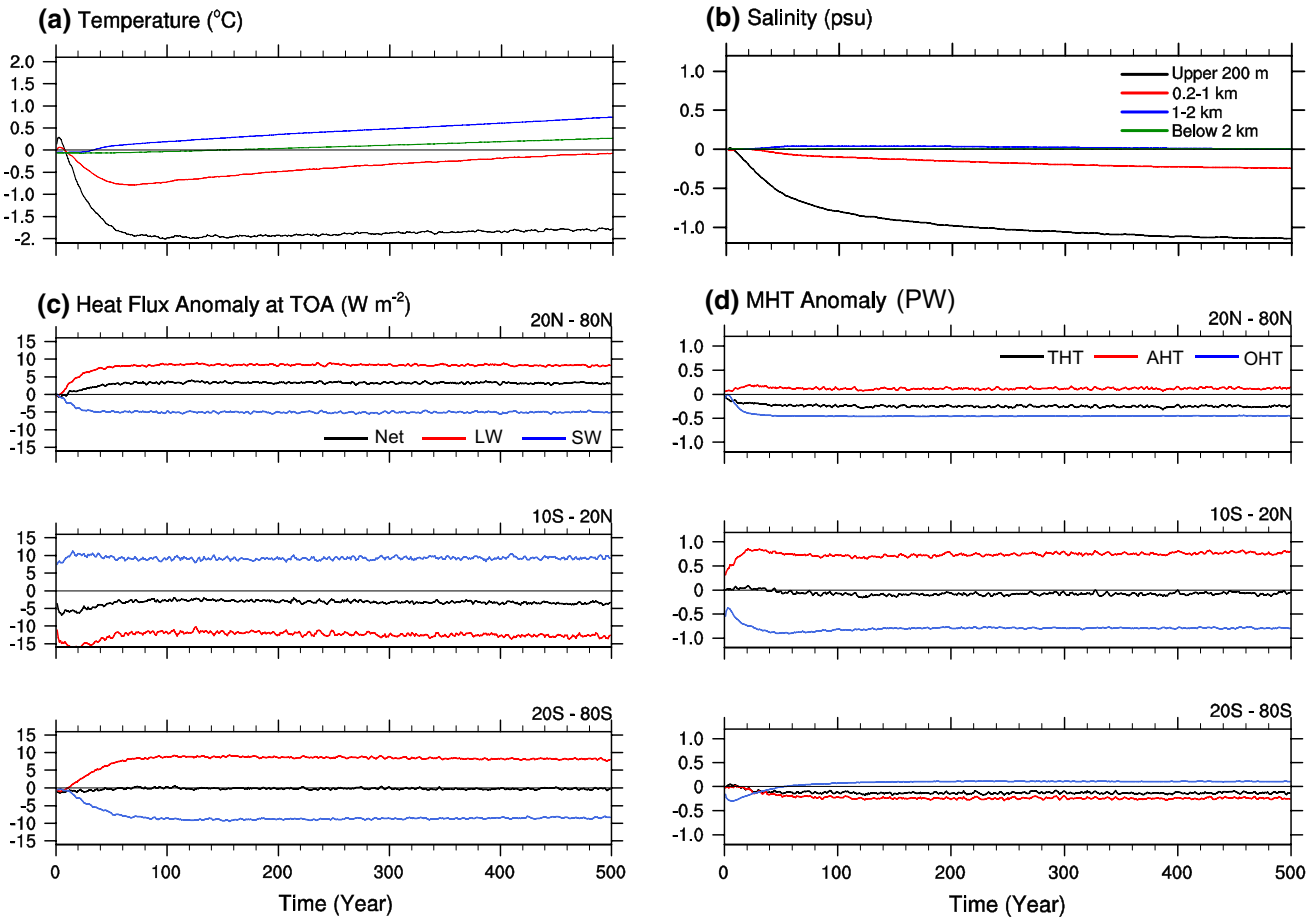

Fig. 1 Temporal evolutions of **a** the global mean oceanic temperature and **b** salinity changes averaged in different depth layer, **c** the net radiation flux change at the top of atmosphere (TOA) and **d** the meridional heat transport (MHT) change averaged in different latitude bands in 0.1 W run. **c** The changes in the net downward shortwave (*SW blue*), net upward longwave (*LW red*) and net radiation flux (*SW plus LW black*) are plotted. Positive values represent net downward flux changes. **d** The total MHT of the Earth system (*black*), the AHT (*red*) and the OHT (*blue*) are obtained from the net radiation flux at the TOA, the net heat flux of the atmosphere and the oceanic velocity–temperature, respectively. All the changes are defined as the differences between the 0.1 W run and the CTRL over the same period. All data are applied by a 10-year running mean

mainly in the mid-high latitudes. The fresher ocean is mainly due to the sea ice melting, which occurs mainly in the North Atlantic and results from the more sea ice output from the Arctic Ocean due to the reduced wind (Fig. 2b). These have been examined in details in Yang et al. (2014b).

The Earth's climate as a whole is determined by the net radiation flux at the TOA, which reaches a quasi-equilibrium in about 50 years, roughly equal to the transient time scale of the global ocean (Fig. 1c). It is seen that the change in the net downward SW radiation and the net outgoing LW radiation at the TOA tend to be in phase in most latitudes. That is, a decrease (increase) in the downward SW can be roughly compensated by a decrease (increase) in the upward LW, leaving a trivial change in the net radiation flux. Conceptually, a decrease in the outgoing LW corresponds to a lower surface temperature, which can result in a larger planetary albedo (for example, more sea ice in the mid-high latitudes, Fig. 2b), and then a decrease in the net downward SW. The compensation effect between the LW and SW at the TOA leads to a reduced change in the net radiation flux, suggesting that the Earth's climate as a whole tends to be steady.

The MHT of the Earth system also reaches quasi-equilibrium at the same pace with the radiation flux at the TOA (Fig. 1d). The local balance of heat flux determines the MHT. Therefore, the timescale of MHT adjustment is also very short and well consistent with that of the net radiation flux in Fig. 1c. The OHT is calculated directly from the meridional velocity and potential temperature, while the AHT here is deduced from the difference of the net radiation flux at the TOA and the net surface heat flux over the ocean, which is not explicitly related to the ocean internal dynamics. It is seen that during the whole evolution period, the changes in the OHT and AHT tend to be out of phase in most regions. They

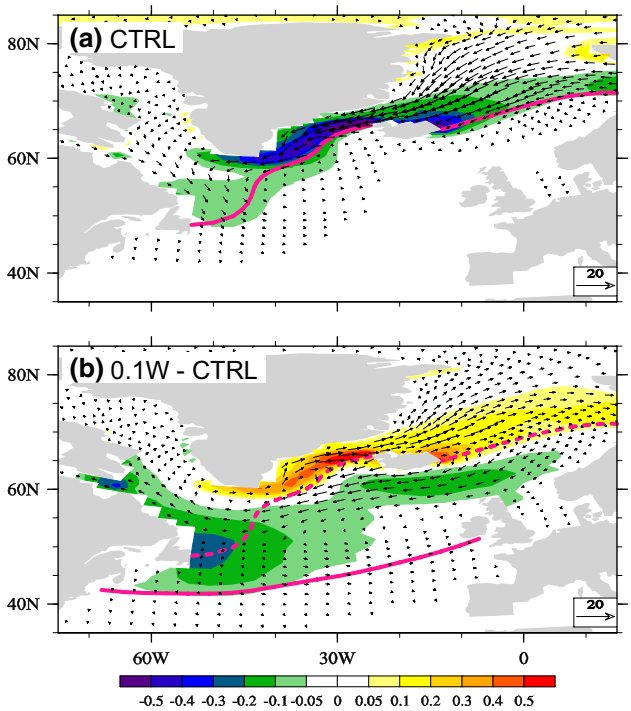

Fig. 2 **a** Annual mean sea ice formation (*colour* psu/month), the sea ice velocity (*vector* cm/s) and the sea ice margin (*red line*) defined as the 15 % sea ice fraction in the Atlantic in the CTRL. The negative sea ice formation represents the sea ice melting, which has been transformed into the virtual salt flux by multiplying $S_0/(\rho_0 H)$, where S_0 (35) is the reference salinity; ρ_0 is the mean sea water density and H is the upper layer depth (30 m). **b** Their changes in 0.1 W run, the *dash* (*solid*) *line* represents sea ice margin in the CTRL (0.1 W run)

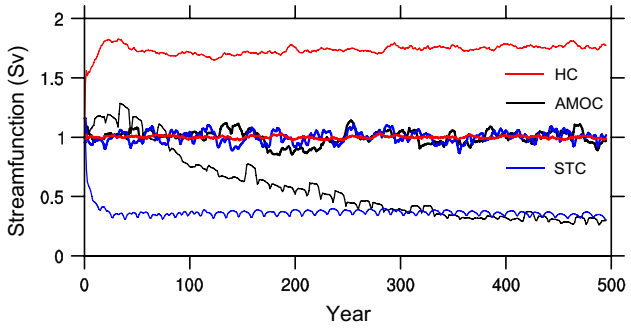

Fig. 3 The indexes of the Atlantic meridional overturning circulation (*AMOC black*), the subtropical cell (*STC blue*) in the Pacific and the atmospheric Hadley cell (*HC red*). The AMOC (STC) index is defined as the maximum value of the streamfunction in the range of 0–10 °C (20–30 °C) isothermal level and 20°–70°N (30°S–30°N) in the Atlantic (Indo-Pacific). The Hadley cell index is defined in the range of 0°–15°N and between 200 and 1,000 hPa. The *bold* (*thin*) *lines* are for the CTRL (0.1 W run). All indexes are normalized by their time-mean maximum values in the CTRL, which are 21, 39 and 93 Sv for the AMOC, STC and HC, respectively. Here 1 Sv is 106 m^3/s for the ocean and 109 kg/s for the atmosphere. A 10-year running mean is used to smooth the curves

have significant negative correlation and compensate with each other to a great extent. There is also non-trivial undercompensation between the AHT and the OHT in high latitudes. The compensation problem is our focus in this work.

Both wind-driven and thermohaline circulations are weakened in the wind runs, while the atmosphere circulation is enhanced. Figure 3 shows that both the subtropical cells (STCs) in the Indo-Pacific and the Atlantic meridional overturning circulation (AMOC) are weakened by nearly 70 %, while the atmospheric HC in the tropics is enhanced by the similar magnitude. The compensation change in the atmosphere and ocean circulations occurs simply as follows: the weakening of ocean meridional overturning circulations results in less poleward ocean heat transport, which in turn leads to tropical warming and extratropical cooling. This enhances the poleward SST gradient and thus the atmosphere circulation. The response timescale of the STC is very short and comparable with that of heat flux. The AMOC timescale is much longer and more related to the evolution of the salinity. The HC timescale is even shorter than that of the STC. It is strengthened by 50 % in the first year, in response to the rapid change in the SST (Figure not shown), where the latter is in turn a result of the weakened ocean circulation. Note that in Fig. 3, the curves are normalized by the mean maximum values of the CTRL, so that the relative changes are clearly demonstrated. More detailed analyses will be presented in the later section.

The mechanisms for the AMOC change (Fig. 3) have been examined in details in Yang et al. (2014b). Briefly, when the wind-stress is reduced, the vertical convection and diffusion are weakened immediately, resulting in a salt deficit in the northern North Atlantic that prevents the deep water formation there. This triggers the AMOC reduction. As the AMOC weakens, the sea ice expends southward and melts (Fig. 2c), freshening the upper ocean that weakens the AMOC further. There is a positive feedback between the sea ice melting and AMOC weakening, which eventually results in the AMOC shutdown. The salinity advection from the south, however, plays a contrary role to the sea ice melting, salting the upper ocean in the North Atlantic between 40° and 60°N (Figure not shown). This is different from previous studies (e.g., Timmermann and Goosse 2004) which emphasize the important role of salinity advection from lower latitudes in the AMOC.

4 Equilibrium responses

4.1 Radiation balance at the TOA

The equilibrium changes in the net SW and LW at the TOA are within the 5–10 % of the total values in 0.1 W run

(Fig. 4). The net radiation flux change is even smaller since the compensation changes between the SW and LW. Figure 4 shows the zonal averaged radiation flux in the CTRL and their changes in 0.1 W run. In the low-mid latitudes (50°S–50°N), the compensation is nearly perfect, leaving the net radiation flux roughly unchanged (Fig. 4b). In this region, cloud feedback plays a dominant role in regulating the radiation flux. In the latitude band of 20°–50°S/°N, a positive LW change (Fig. 4b) represents a reduced outgoing LW caused by the lower SST. More stratus clouds and more equatorward sea ice output from the polar region increase the planetary albedo (Figure not shown), resulting in a less downward SW. In the low latitudes (20°S–20°N), it is interesting to see the LW (and SW) change itself has different sign in the different sides of latitude 8°N. 8°N is the mean ITCZ latitude in the CTRL. The ITCZ shifts southward towards the equator in 0.1 W run in response to the higher SST on the equator. The outgoing LW is reduced (positive change) to the south because of an increase in mid-high clouds, as a result of stronger convection due to the higher SST. This also increases the albedo here and reduces the downward SW. To the north of 8°N the deep convection, and thus the mid-high clouds, is reduced due to the southward shift of ITCZ. This increases the outgoing LW (negative) and the downward SW. In general, the opposite change in the LW (SW) in the tropics is determined by the shift of ITCZ, which leads to nearly perfect compensation between the SW and LW at the TOA. Overall the global net radiation flux change is trivial. It is only 0.3 W/m^2 in 0.1 W run, roughly about 0.1–0.3 % of the total values, much weaker than the net radiation change caused by the greenhouse gas change during the past 100 years (around 1.6 W/m^2) (IPCC 2007). We conclude that the overall Earth's climate in the reduced wind runs does not change too much, however, significant changes may occur in the ocean and atmosphere components.

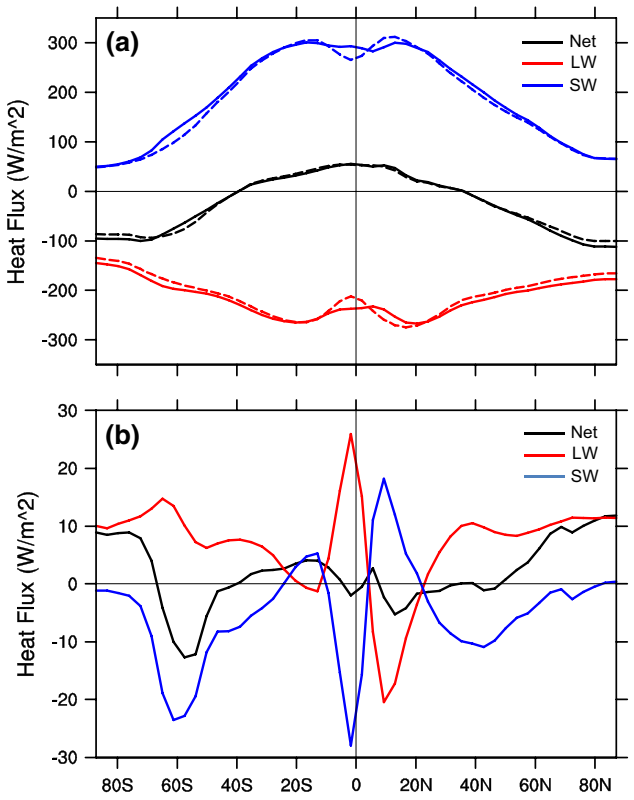

Fig. 4 **a** The net radiation flux (*black*), the net downward SW (*blue*) and net outgoing LW (*red*) at the TOA. *Solid lines* for the CTRL and dashed lines for 0.1 W run. **b** The changes of the TOA net radiation flux in 0.1 W run. *Black*, *blue* and *red lines* are for net total, SW and LW changes, respectively. The mean values from the CTRL have been subtracted. Unit: W/m^2

4.2 Changes in the MHT

The changes in the AHT and OHT are the main focus of this work. We will further delve into the mechanisms on the relationship between their changes. The mean MHT is briefed here first. The equilibrium Earth is maintained by nearly hemispherically antisymmetric MHT, with the peak poleward transport occurring around 40°N/S (Fig. 5a). The AHT dominates the MHT poleward of about 10°N/S while the OHT dominates in the deep tropics. These features are consistent with previous studies (e.g., Trenberth and Caron 2001). In 0.1 W run, significant changes occur in both the AHT and OHT, with the peak change of around 1.4 PW. The OHT is reduced while the AHT is enhanced, exhibiting compensation feature in most latitudes (Fig. 5b). This leaves the total MHT change much suppressed, with a peak change of around 0.6 PW near 40°N. Specifically, in the tropics (30°S–30°N), there are good compensation between the changes in the OHT and AHT. The compensation rate (CR), defined as the residual of the ratio of the net MHT changes to the maximum changes in the OHT and AHT (Swaluw et al. 2007), reaches 80 % in the deep tropics (Fig. 5d). In the extratropics, the CR drops quickly from nearly 40 % in the 30°N/°S to nearly (even below) zero in the 40°N (40°S). In the high latitudes, the situation is more complicated. In the northern high latitudes the AHT change is small and has the same sign as the OHT change. In the southern latitudes of Antarctic circumpolar current (ACC), the CR peaks at 60 %. In general, we see good compensation in the tropics and big undercompensation of the AHT to the OHT in the high latitudes, particularly in the NH. This work investigates both the compensation and un-compensation mechanisms.

The compensation change between the AHT and OHT is consistent with that between the atmospheric and oceanic overturning circulations shown in Fig. 3. Here the components of OHT are examined. It is seen that the OHT changes in the Indo-Pacific and Atlantic are comparable (Fig. 5c). In 0.1 W run, the total OHT change peaks about 1.3 PW near 20°N (Fig. 5b), in which about 0.8 PW

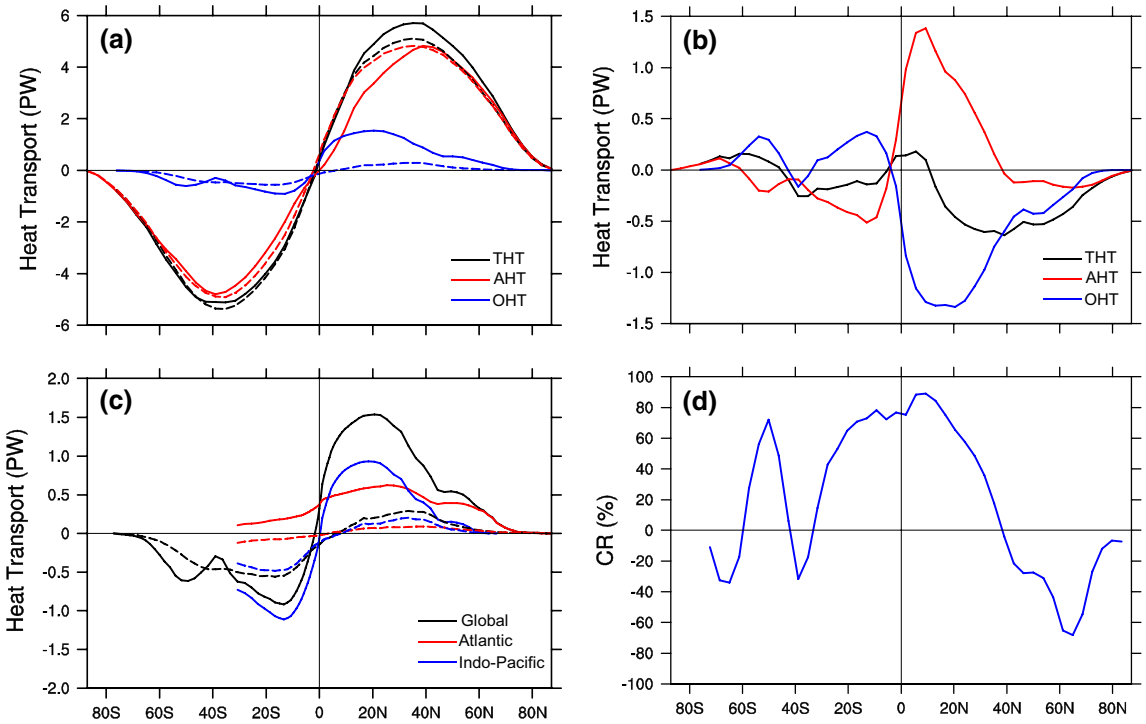

Fig. 5 **a** The total MHT (*black*), AHT (*red*) and OHT (*blue*) in the CTRL (*solid lines*) and 0.1 W run (*dashed lines*) and **b** their changes in 0.1 W run. **c** The OHT in the CTRL (*solid lines*) and 0.1 W run (*dashed lines*). *Black*, *red* and *blue lines* are for the global ocean, the Atlantic and the Indo-Pacific, respectively. **d** The compensation rate between the changes in the AHT and OHT (unit: %), see text for definition

reduction occurs in the Indo-Pacific, representing a maximum 80 % reduction in the Indo-Pacific OHT (Fig. 5c). The remaining 0.5 PW reduction occurs in the Atlantic, which is almost equivalent to the shutdown of the Atlantic OHT. These reductions are consistent with the significant weakening of the STC and AMOC (Fig. 3). Actually, the Indo-Pacific (Atlantic) OHT can be roughly thought as the contribution by wind-driven (thermohaline) circulation. In 0.1 W run, the OHT reduction in the tropics (0.8 PW) is mainly attributed to the change in wind-driven circulation. While in mid-high latitudes, the thermohaline OHT change (0.5 PW) dominates (Fig. 5c).

4.3 Changes in the ocean temperature, salinity and density

As a consequence of reduced OHT, the poleward temperature gradient is enhanced substantially, with the significant cooling off the equator and warming along the equator (Fig. 6a, b). The equatorial warming occurs mainly in the cold tongue region of the Pacific because of the ceasing of the upwelling there as a result of the termination of equatorial trade winds. The equatorial warm pool, instead, cools slightly because the termination of the westward surface warm water advection dominates against the less poleward Ekman transport. The zonal SST gradient is weakened, so is the Walker circulation (Fig. 12). In the off-equator, the SST cooling is due to the less poleward Ekman transport. In the high latitudes, the surface cooling can be significant, more than 8 °C cooling in the high latitudes North Atlantic in 0.1 W run. It is seen that the SST change in the NH is much stronger than that in the SH, showing an asymmetric pattern (Fig. 6b). This results from an asymmetric change in the OHT (Fig. 5c), and will further result in an asymmetric change in the HC. The annual mean ascending latitude of the HC is shifted southward from 10°N to around the equator. In addition, the HC becomes stronger due to enhanced poleward SST gradient, which furthermore enhances the baroclinicity in the atmosphere, resulting in more eddy activities and a poleward E–P flux and thus a stronger poleward AHT in 0.1 W run. We will have more discussions later.

The sea surface salinity (SSS) is also reduced remarkably throughout the whole ocean surface (Fig. 6c, d). Overall the ocean gains fresh water in the reduced wind experiments. The SSS is reduced by more than 6 psu in the North Atlantic in 0.1 W run (Fig. 6d). This eventually determines the density in the high latitudes. The sea ice plays a key role here in the ocean freshening. The total sea ice melting to ocean is nearly doubled in 0.1 W run, increasing from 0.43 Sv in the CTRL to 0.81 Sv in 0.1 W run (Figure not shown). The enhanced

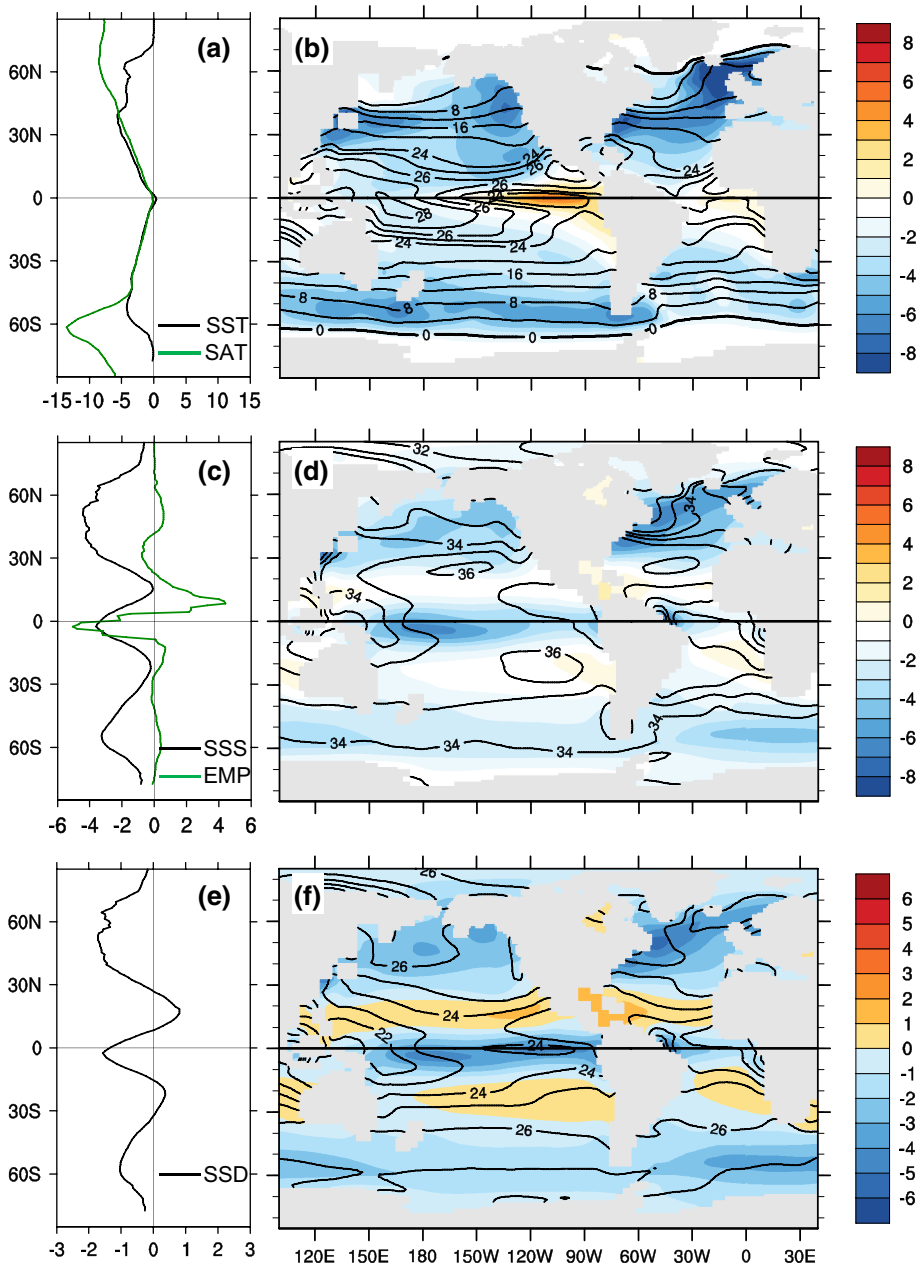

Fig. 6 (*Upper*) **b** The mean sea surface temperature (*SST*, *contour*, CI = 1 °C) in the CTRL and the SST change (*color*) in 0.1 W run. **a** The zonal mean SST (*black*) and SAT (*green*) changes in 0.1 W run. (*Middle*) Same as the upper panels but for **d** the mean sea surface salinity (*SSS*, *contour*, CI = 1 psu) and its change (*color*), as well as **c** the zonal mean SSS (*black*) and EMP (*green* mm/day) changes. (*Lower*) **f** the mean sea surface density (*SSD*, *contour*, CI = 1 kg/m^3) and its change (*color*), as well as **e** its zonal mean change (*black*)

melting results from the more equatorward ice transport from the high latitudes North Atlantic (Fig. 2b). The significant weakening in the ocean circulations results in more sea ice output to the lower latitudes and thus melting. The freshening in the poleward of 40°S is due to less saline water upwelling in the Southern Ocean. In the deep tropics 10°S–10°N, the freshening is mainly due to more precipitation, associated with the stronger convection due to warmer SST.

The surface density change shows a similar pattern to that of SSS (Fig. 6f). The high latitude freshening effect overcomes the cooling effect on the density, resulting in a decrease in the surface density. In the deep tropics (10°S–10°N), the surface density reduces due to both the freshening and warming. In the subtropics (10°–30°N/S), the surface density increases slightly due to colder SST. In general, it is the surface salinity change that eventually contributes to the weakening of the AMOC and thus the reduced poleward OHT. This might imply a critical role of the hydrological cycle in the OHT, and further in the stability of the Earth energy balance. We will pursue this problem in our future work.

The changes in the ocean interior are also checked here. The strong surface cooling can penetrate downward to 500 m. There is also strong warming occurring beneath the mean thermocline (Fig. 7a, b). In the tropics the subsurface warming is caused by the weakening of the equatorial Ekman upwelling and surface Ekman

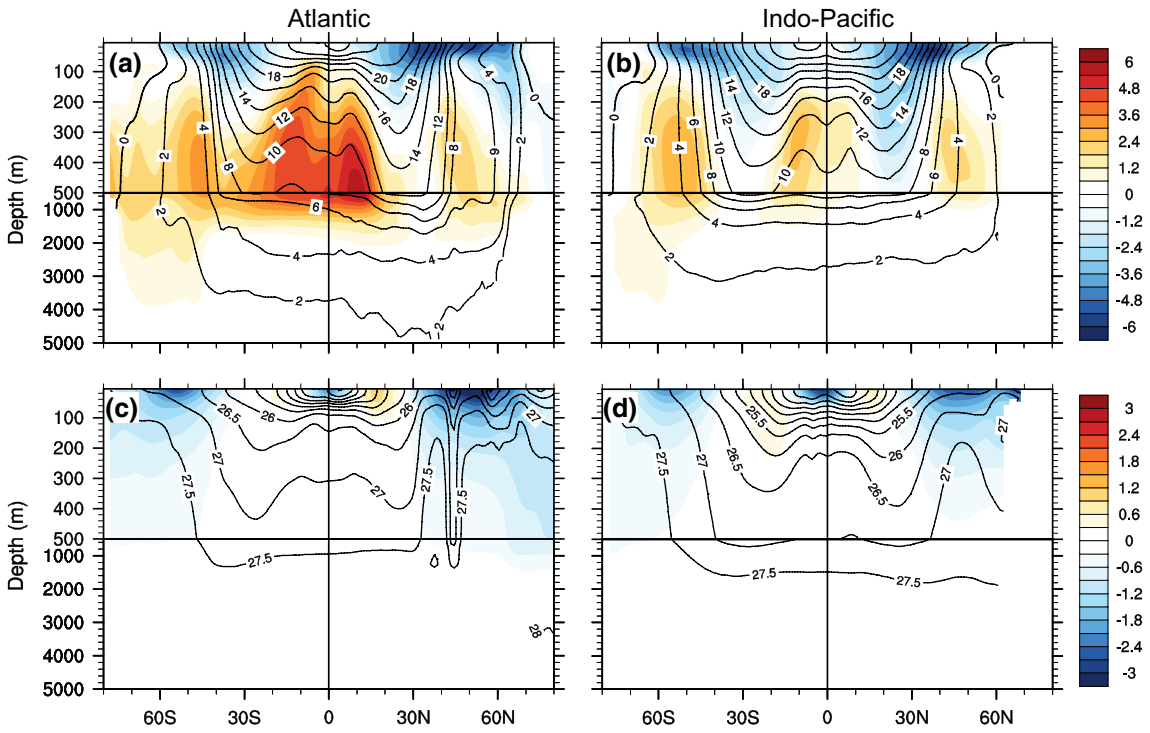

Fig. 7 The changes in **a**, **b** temperature (*color* °C) and **c**, **d** density (*color* kg/m^3) in the Atlantic (*left*) and Ind-Pacific (*right*) in 0.1 W run, superimposed by the mean temperature and density (*contours*) in the CTRL

divergence, as well as the downward displacement of the equatorial thermocline, consistent with the weakening of the STC and AMOC. The stronger warming in the Atlantic is due to the combined effect from both the STC and AMOC weakening. While in the Pacific the weaker warming is due solely to the STC (Yang and Wang 2011). In the subpolar region (40°–60°N) the warming is due to the baroclinic response (Chang et al. 2008). The surface cold water can not affect the subsurface due to the shutdown of the AMOC. The subsurface ocean then warms due to the water column stretch. In general, the vertical temperature stratification in global oceans is weakened, which also contributes to the decrease of the OHT (Yang et al. 2013).

The density changes in the ocean interior (Fig. 7c, d) almost resemble the surface density changes (Fig. 6f), which is roughly barotropic kind. The density changes in the Atlantic and Indo-Pacific are similar. The extratropical density (30°N/S poleward) decreases significantly from the surface to around 500 m depth, which is mainly caused by the freshening in the upper oceans as discussed above. The meridional density gradient is thus weakened significantly. This is particularly clear in the Southern Ocean region (40°–80°S) (Fig. 7c, d), where the isopycnal levels become nearly flat in the upper ocean in 0.1 W run due to 2–3 kg/m^3 decrease. The meridional density gradient is closely related to the bolus overturning circulation associated with meso-scale eddies (Marshall and Radko 2003), which is opposite to the Eulerian mean overturning circulation. The flattening of the isopycnal level will reduce the bolus circulation and thus the associated OHT.

4.4 Changes in the MOC and OHT

The MHT change is the central concern in this work. Here the ocean mass transport in the potential temperature–latitude space is examined first (Fig. 8), because the heat transport is eventually determined by the temperature difference between the upper northward flow and lower return flow (Held 2001). The "net" meridional overturning circulation (MOC) (Fig. 8a) is the residual of the Eulerian mean circulation (Fig. 8b), the circulations caused by meso-scale (Fig. 7c) and submeso-scale eddies (Fig. 8d). Their physics have been discussed in details in many previous studies (Marshall and Radko 2003; Fox-Kemper et al. 2008). The Eulerian mean MOC dominates (Fig. 8b). The bolus circulation is induced by mean buoyancy gradient and parameterized by Gent–McWilliams scheme (Gent and McWilliams 1990). It is important in the ACC region and northern mid-latitudes subduction region (Fig. 8c), in association with the strong (weak) meridional (vertical) buoyancy gradient. The overturning circulation associated with submeso-scale eddies is mainly confined in the mixed layer (Fig. 8d), which

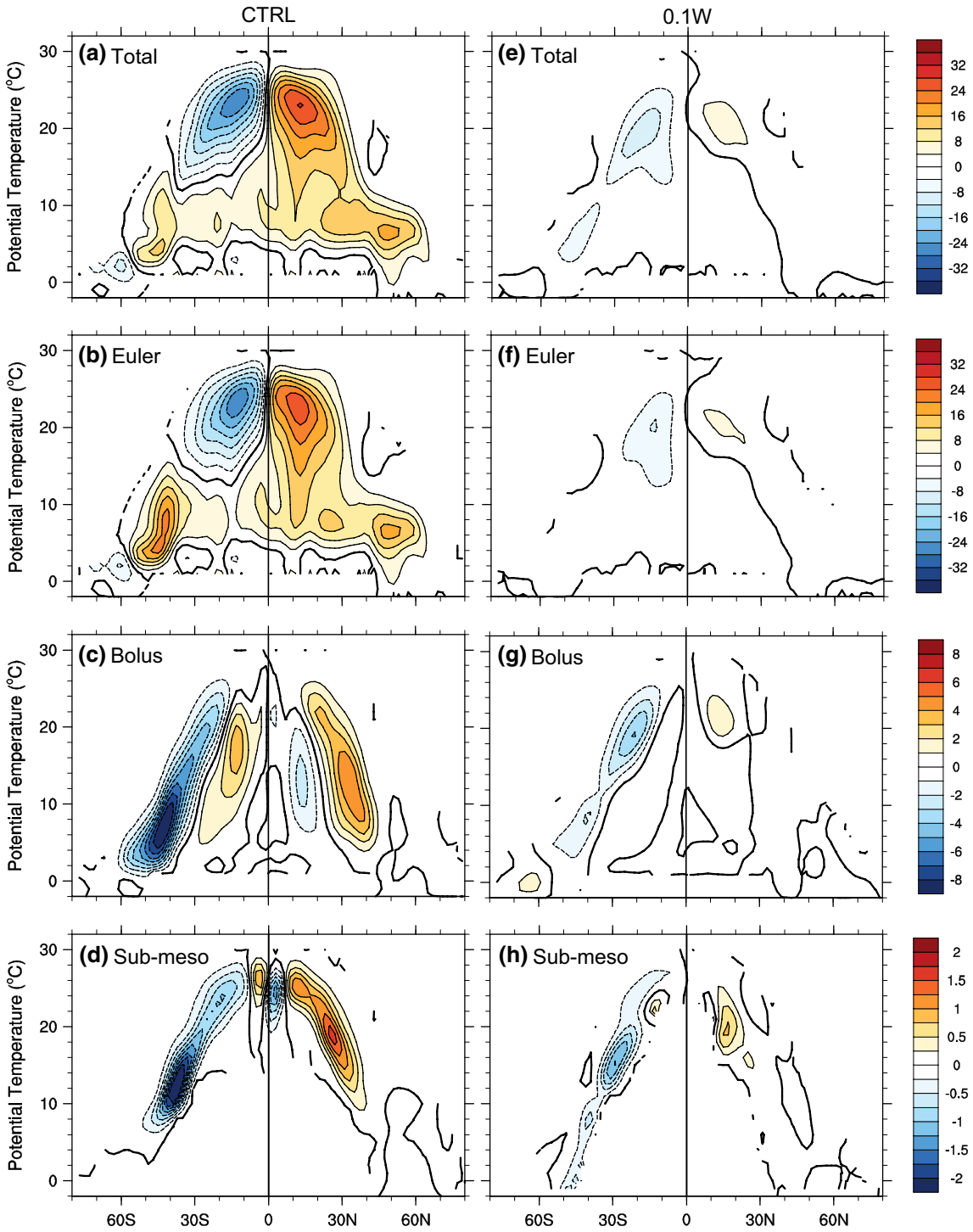

Fig. 8 The mean mass stream function (*color* Sv) in (*left*) the CTRL and (*right*) the 0.1 W run in the potential temperature–latitude coordinate. The total mass stream function (**a**, **e**) is the residual of the Euler mean (**b**, **f**), the bolus (**c**, **g**) and the submeso-scale (**d**, **h**) components

depicts the restratifying effect on the mixed layer and is parameterized by the FFH scheme (Fox-Kemper et al. 2008, 2011; Fox-Kemper and Ferrari 2008). The maximum of this term can be one-fifth of the Eulerian mean circulation in the mixed layer. In the temperature-latitude space, the wind-driven STC and AMOC are well separated. The warm cells (the wind-driven) in both hemispheres span the temperature ranging from 12 °C in the mid-latitude 40°–50°N/°S to near 30 °C at the equator (Fig. 8a, b). The cold cell, that is, mostly the AMOC

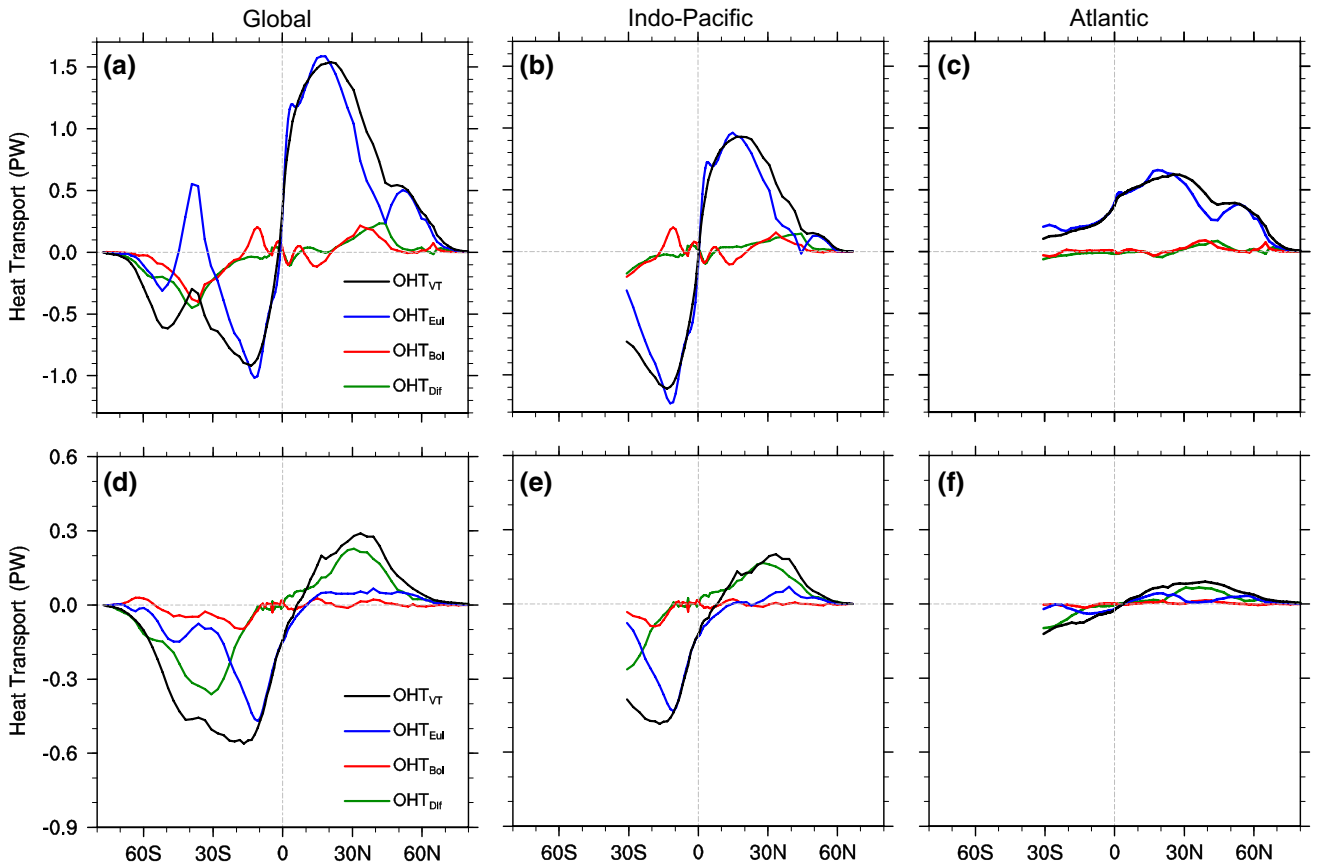

Fig. 9 (*Upper*) The mean meridional OHT (PW) in **a** the global ocean, **b** the Indo-Pacific and **c** the Atlantic in the CTRL. The total OHT (*solid black*) is decomposed into the contributions from the Euler mean current (*blue*), the bolus cell (*red*) and the dissipation (*green*). (*Lower*) **d**–**f** Same as the upper panels but for those in 0.1 W run

spans the temperature from 2 to 10 °C, which is mainly confined in the NH.

In 0.1 W run, all four components of the MOC are reduced significantly (Fig. 8e, f). The Eulerian mean circulation is reduced by the 80 %, in which the wind-driven part is decreased from 32 to 8 Sv and the AMOC is reduced from 20 to <4 Sv. The bolus circulation is also reduced by 80 % from the maximum 8 to <2 Sv, as a result of the flattening of the isopycnal level in the Southern Ocean. A similar situation occurs to the mixed layer submeso scale circulations, which is due to the weakening of wind-induced vertical mixing.

Consequently, the changes in the OHT components can be quantified here. They are determined by the changes in the MOC components. Both the Eulerian mean OHT and bolus OHT are reduced significantly as expected. The poleward OHT is however sustained by the dissipation OHT in most latitudes. As seen before, the total OHT reduction peaks about 1.3 PW near 20°N (Fig. 5b). Although the ocean circulations are weakened by more than 80 %, the remaining OHT is still remarkable in 0.1 W run. It still has around 0.5 PW poleward heat transport left in the SH. Figure 9 shows the OHT and its components in different basins in the CTRL and 0.1 W run. The total OHT_{VT} is the sum of advective (OHT_{ADV}) and dissipation (OHT_{Diff}) heat transport, in which the OHT_{ADV} includes contributions from Eulerian mean circulation OHT_{Eul}, mesoscale eddies OHT_{Bol}, submeso-scale eddies OHT_{Sub}. The OHT_{Sub} is too small (not plotted in Fig. 9) since it is within the mixed layer where the temperature is nearly uniform. The OHT_{ADV} eventually consists of OHT_{Eul} and OHT_{Bol}. The OHT_{Eul} (blue, Fig. 9a) can represent the OHT_{VT} very well in most regions, except that in the Southern Ocean both the OHT_{Bol} and OHT_{Diff} are however significant, consistent with the sharp poleward temperature gradient. It is noticed that in this region, in association with the strong northward Ekman flow driven by furious westerlies, the OHT_{Eul} is northward with the peak value of 0.3 PW, while the OHT_{Bol} and OHT_{Diff} are southward, with the peak values of −0.3 and −0.4 PW respectively, reversing the OHT_{Eul} and eventually determining the poleward heat transport (Fig. 9a). In 0.1 W run, the OHT_{Diff} is hardly changed and stands out to be the main component

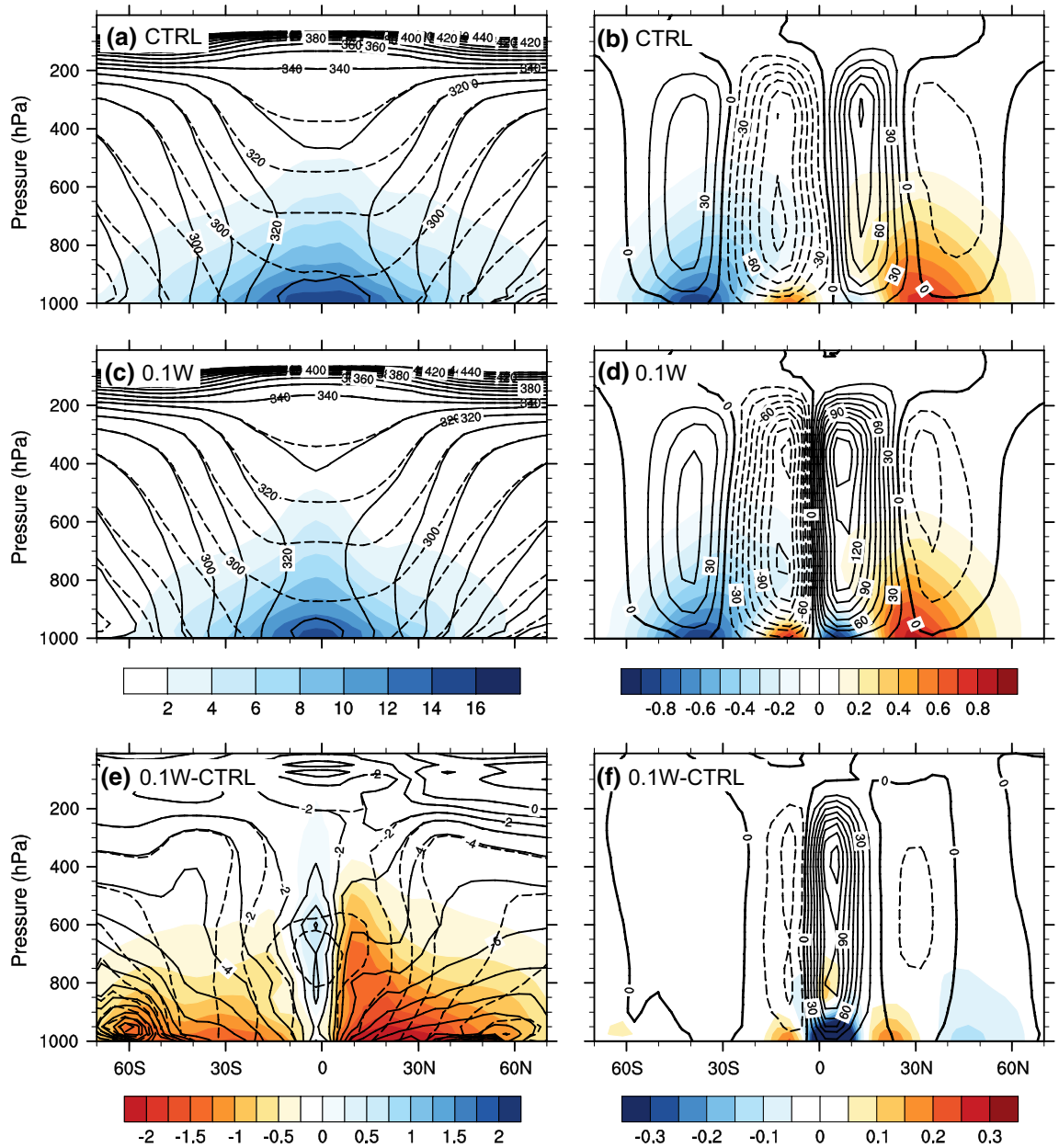

Fig. 10 (*Left*) The mean moist potential temperature (*solid line* K), dry potential temperature (*dashed line*) and specific humidity (*color* g/kg) in **a** the CTRL and **c** 0.1 Wrun, as well as **e** their changes in 0.1 W run. (*Right*) The mean atmospheric meridional mass stream function (*contours* 109 kg/s) and water vapour transport (*color* 109 kg/s) in **b** the CTRL and **d** 0.1 W run, as well as **f** their changes in 0.1 W run

in transporting heat poleward (Fig. 9d). The OHT_{Eul} is weakened substantially and the OHT_{Bol} nearly disappears. Notice that the OHT_{Eul} still has about 0.4 PW left at 10°S (Fig. 9d, e), which is due to the remaining STC in the southern Indo-Pacific (Fig. 8e, f). It is further seen that in the reduced wind world, the Indo-Pacific plays a more significant role in poleward heat transport (Fig. 9e, f). For the detailed calculation of the OHT components, please refer to Yang et al. (2014a).

4.5 Changes in atmosphere static energy, mass transport and water vapour transport

Before discussing the AHT change, we first examine the atmosphere energy and mass transport separately. The atmosphere moist static energy (MSE), the DSE and specific humidity are shown in Fig. 10a. The MSE is represented by the moist potential temperature, which includes the atmosphere internal energy, the latent energy (LE)

related to the water vapour and the geopotential energy (Czaja and Marshall). The DSE excludes the latent energy. It is seen that in the tropics (within 30°N/S) the MSE is nearly vertically homogeneous below 200 hPa because of the strong water vapour latent heat release (Fig. 10a). The difference between MSE and DSE suggests the contribution of the moisture to the tropical heating, which is over 30 K in the lower atmosphere (below 800 hPa) and 10 K in the upper layer (above 750 hPa). It is well-known that the tropical ocean provides the most water vapour to the atmosphere, which supplies the lower tropical atmosphere with more than 10 g moisture for 1 kg atmosphere (Fig. 10a). The moisture effect on the potential temperature diminishes toward the high latitudes (poleward of 30°N/S) as well as the top of troposphere.

The mass transport and water vapour transport are shown in Fig. 10b. The mean meridional mass transport, represented mostly by the HC, is opposite to the water vapour transport in direction, with the magnitude of the former about 100 times of the latter. The water vapour is transported by the equatorward convergent flow in the lower troposphere, that is, the lower branch of the HC in the tropics, enhancing the tropical convection through the latent heat release. It is worth noting that although the water vapour mass transport is two-order smaller in magnitude than total air mass transport, the water vapour is 100 times more efficient than dry air in transporting heat (Huang 2005). One kilogram of water vapour can deliver 2.5×10^6 J of heat (the latent heat content of water vapour $L_e \sim 2.5 \times 10^6$ J/kg), but one kilogram of air (water) can only release 10^4 J (4.18×10^4 J) of heat for a 10 °C cooling. This makes the atmospheric latent energy transport significant in the climate system. The water vapour transport in Fig. 10 is directly calculated based on the model output of vq. In the tropics it is accomplished by the mean circulation (i.e., the HC), while in the extratropics (poleward of 25°N/S) it is fulfilled mostly by the eddy activities, because the v in the vq represents mainly the HC in the tropics and then eddies in the extratropics. It is seen that the mean water vapour transport in the tropics is opposite to and also much weaker than the eddy water vapour transport in the extratropics (Fig. 10b).

The atmospheric becomes drier and its baroclinicity becomes stronger in 0.1 W run (Fig. 10c, e). These changes are very clear in the off-equator, where the lower atmosphere is about 20 % drier and the atmospheric baroclinicity ($\partial T/\partial y$) is enhanced by more than 30 %. This implies that the poleward latent heat transport will be decreased in the extratropics while the poleward eddy heat transport will be enhanced. Figure 10e shows the changes in the atmospheric potential temperature and the specific humidity in 0.1 W run. The stronger convection at the equator increases the humidity from the surface to the upper troposphere, but this is constrained within 5°N/S of the equator. Where else the water vapour decreases significantly, consistent with the colder SST that reduces the evaporation. The lower level atmospheric temperature is reduced by as much as 10 K in the mid-high latitudes, which at the same time enhances the atmospheric baroclinicity greatly. The HC is enhanced by 80 % and its ascending branch shifts southward to the equator (Fig. 10d, f) in 0.1 W run, showing a more symmetric structure in the atmospheric circulation. Consequently, the equatorward water vapour transport is enhanced. The eddy water vapour transport in the mid-high latitude is weakened slightly (Fig. 10f).

4.6 Changes in the AHT

The change in the AHT can be considered as the integral projection of those atmospheric changes discussed above. Compared to the CTRL, in 0.1 W run the poleward mean (eddy) DSE transport is enhanced by as much as 60 % (40 %) in the tropics (midlatitudes). And the equatorward LE transport is more than doubled. Figure 11 shows the components of AHT and their changes. The detailed calculations of these components can be found in our recent paper (Yang et al. 2014a). In Fig. 11a–c, the AHT is decomposed into DSE transport (AHT_{DSE}) and LE transport (AHT_{LE}). In the deep tropics within 20°N/S, the AHT_{LE} acts against the AHT_{DSE}, reducing the heat loss towards high latitudes (Fig. 11a, b). Consistent with the mass transport shown in Fig. 10b and d, the equatorward AHT_{LE} carried by the lower branches of the HC converges at the latitude of ITCZ. In the tropics, the AHT_{LE} under-compensates the AHT_{DSE}, while in the mid-high latitudes (30°–60°N/S) the AHT_{LE} acts together with the AHT_{DSE}, contributing as much as one second of the total poleward AHT (Fig. 11a, d), particularly in the SH where the peak AHT_{LE} (2 PW) is about twice of the global OHT at the same latitudes, suggesting the critical role of the water vapour in the Earth heat balance. In 0.1 W run, both the poleward AHT_{DSE} and equatorward AHT_{LE} increase significantly, which mainly occur in the NH with the peak AHT_{DSE} (AHT_{LE}) enhanced by 3.0 PW (2.0 PW) in the deep tropics (Fig. 11c). Much of them are cancelled with each other, leaving the net change of 1.0 PW in the poleward AHT. It is seen that the compensation changes in AHT_{DSE} and AHT_{LE} occur almost in all latitudes, although they are of a same sign in some latitudes. These changes are consistent with the discussion in Fig. 10. In general, due to the southward shift of the ITCZ, the peak changes in AHT components occur right on the previous latitude of ITCZ. Consistent with the new ITCZ position, the atmosphere has to increase the northward heat transport, to compensate the heat loss in the NH due to the less northward OHT (Marshall et al. 2013). This also explains the asymmetric changes in the SST and SAT

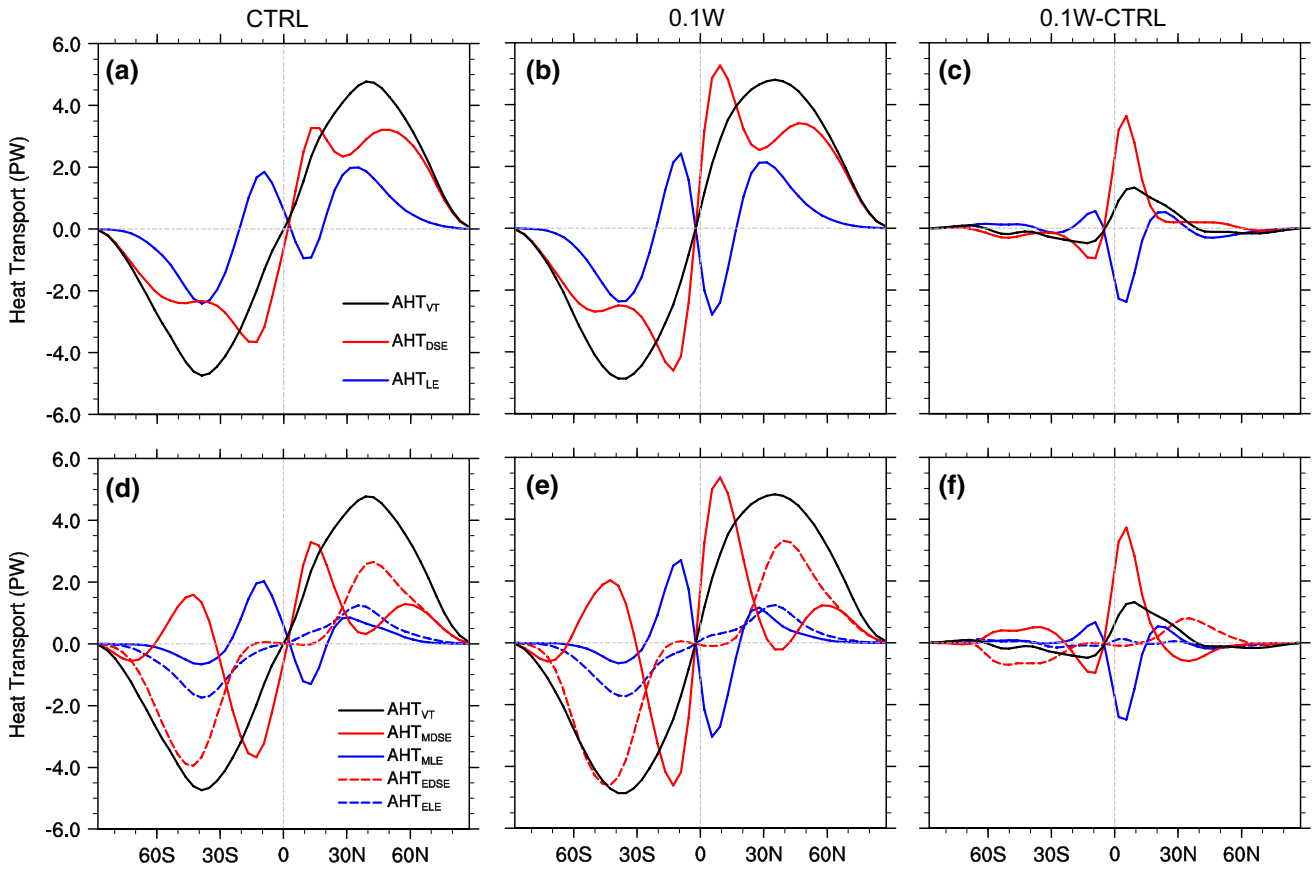

Fig. 11 The AHT (PW) calculated directly from the velocity and temperature. **a**, **d** Are for the CTRL, **b**, **e** are for 0.1 W run, **c**, **f** are for the changes in 0.1 W run. **a–c** The total AHTVT (*black*) is decomposed into the dry static energy (DSE) transport (*AHTDSE red*) and latent energy (LE) transport (*AHTLE blue*). **d–f** The AHT is further decomposed into the mean DSE (*AHTMDSE solid red*), the eddy DSE (*AHTEDSE dashed red*), the mean LE (*AHTMLE solid blue*) and eddy LE (*AHTELE dashed blue*)

shown in Fig. 6c. The SST cooling in the NH is bigger than that in the SH due to the overall southward OHT anomaly, while the SAT drops more in the SH than in the NH due to northward AHT anomaly. This can be seen more clearly in Fig. 13a.

The eddy AHT change dominates the poleward AHT anomaly in the mid-high latitudes (Fig. 11f), which is caused by the enhanced baroclinicity as shown in Fig. 10e. It is well-established that the mean circulation dominates in the tropics and eddies dominates in the mid-high latitudes (Fig. 11d, e). The eddy LE transport AHT_{ELE} is always poleward. It is small and opposite to the mean LE transport AHT_{MLE} in the tropics. The AHT_{ELE} increases towards the higher latitudes, exceeds the AHT_{MLE} poleward of 30°N/S and peaks at around 40°N/S. The eddy DSE transport AHT_{EDSE} is nearly zero in the tropics and increases rapidly towards the higher latitudes, in accompany with the rapid diminishing of the mean DSE transport AHT_{MDSE}. The AHT_{EDSE} accounts to more than 50 % (80 %) of the total AHT in the NH (SH) mid-latitudes. Here the eddy transport includes those from both the stationary waves and transient eddies. The detailed calculations of these terms as well as the analyses can be found in Yang et al. (2014a). In 0.1 W run, the eddy contribution to the AHT comes mainly from the AHT_{EDSE} while the AHT_{ELE} is hardly changed (Fig. 11f). The enhanced AHT_{EDSE} is due to the stronger baroclinicity as shown in Fig. 10e. The negligible change in the AHT_{ELE} is due to drier lower atmosphere, despite the stronger eddy activities. It is interesting to see the changes in the AHT_{EDSE} and AHT_{MDSE} tend to compensate with each other in the off-equator (20°N/S poleward), which makes the total AHT changes in the extratropics negligible. And this eventually results in under-compensation to the OHT change (Fig. 5b).

4.7 Changes in the ITCZ and atmosphere circulations

The equatorward shift of ITCZ position in 0.1 W run is illustrated clearly in Fig. 12. This shift occurs mainly in the Pacific. Figure 12 shows the surface pressure and winds as well as the geopotential height and winds on the 200 hPa level. Following the conventional approach, the ITCZ

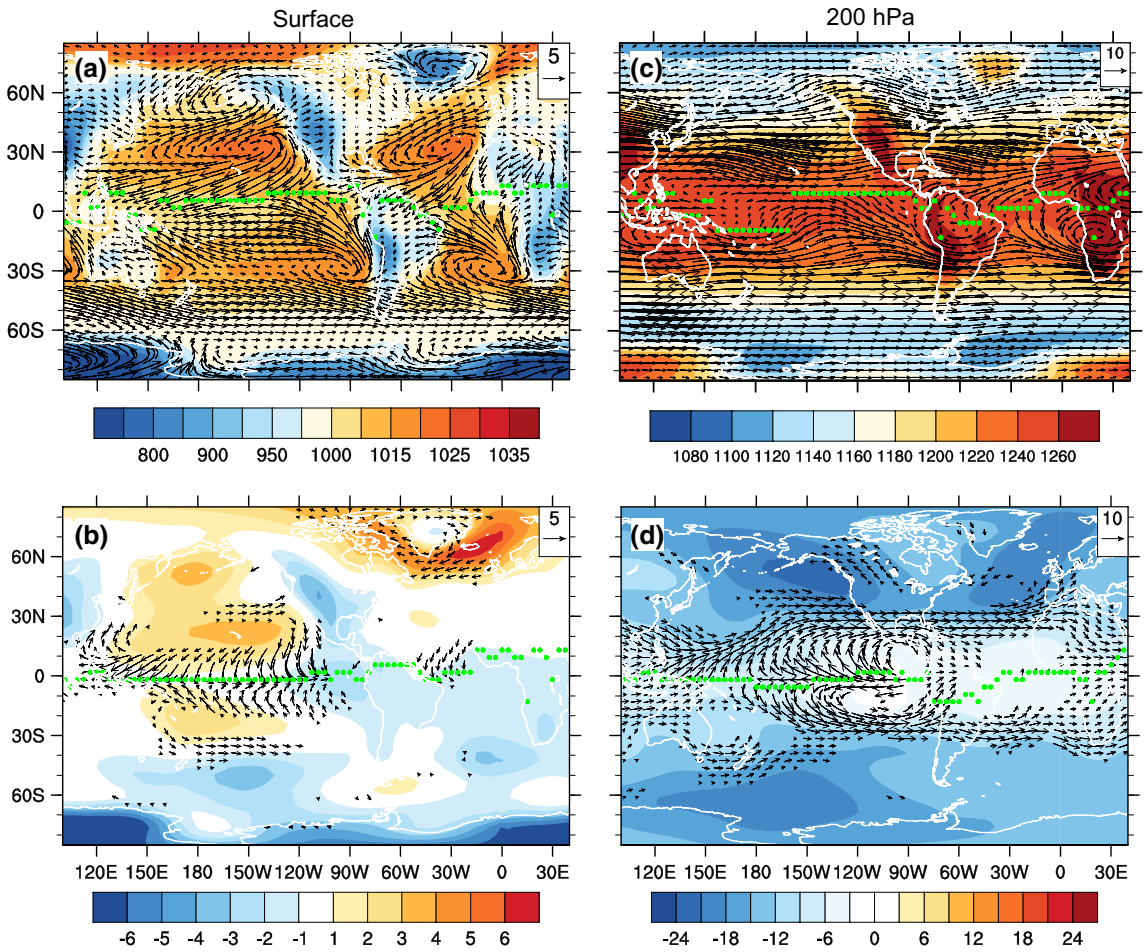

Fig. 12 (*Left*) The mean surface wind (vector, m/s) and surface pressure (*contour*, hPa) in **a** the CTRL and **b** their changes in 0.1 W run. (*Right*) **c**, **d** Same as the left panels but for 200 hPa wind and geopotential height (10 m). **a**–**d** The location of ITCZ is marked as the *green dots*, which is defined as the location of the maximum convergence (*divergence*) of the surface winds (200 hPa winds). The wind changes <1 m/s in **b** and 2 m/s in **d** are not plotted

position is defined as the latitude of the maximum convergence (divergence) of the surface wind (200 hPa wind) (Philander et al. 1996). The green dots in Fig. 12 show the ITCZ position. In 0.1 W run, the wind converges (diverges) right at the equator on the surface (200 hPa) (Fig. 12b, d). The surface pressure shows asymmetric changes. In the NH ocean surface, the Subtropical High is enhanced and both the Aleutian and Polar Lows are weakened in response to the strong cooling in the SST. In the SH ocean surface, the pressure is general lowered.

The AHT change occurs mainly over the tropical Pacific and extratropical Atlantic. This is deduced from the changes in the surface winds and pressure, which provide clues on the relative roles of the different basins in the global AHT change (Fig. 12b). In response to the SST change, the change in surface winds is strongest over the tropical Pacific within 20°N/S and the change in surface pressure is strongest over the high latitudes Atlantic. This suggests that the AHT change associated with the HC shift occurs mainly over the tropical Pacific, and that associated with stronger eddy activities occurs mainly over the North Atlantic. This can be further confirmed by the net heat flux change in the Atmosphere (Figure not shown), which illustrates two important regions: one is located in the eastern tropical Pacific (cold tongue region) with a maximum change of 80 W/m^2; the other is located over the North Atlantic (50°–70°N) with a −80 W/m^2 change. This enhances our fundamental understating on the ocean basin in the global atmospheric heat budget. Furthermore, the atmospheric change over the tropics appears to be barotropic-like, since the wind change in the upper troposphere is similar but of opposite sign to that over the surface (Fig. 12b, d). The change in eddy activities over the North Atlantic is mainly contained in the lower troposphere, which is consistent with the strong baroclinic change in the wind and pressure fields. It is seen that the geopotential

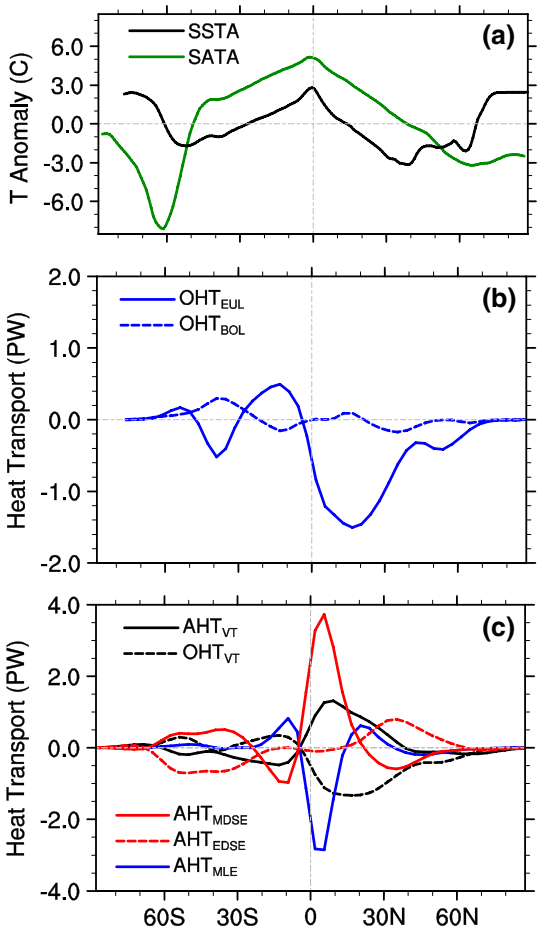

Fig. 13 **a** The zonal mean SST (*black*) and SAT (*green*) changes in 0.1 W run. The meridional mean values are removed for better showing the meridional temperature gradient. **b** The Euler mean (*solid blue*) and the bolus OHT (*dashed blue*) changes in 0.1 W run. **c** Same as **b** but for AHTVT (*solid black*), AHTMDSE (*solid red*), AHTEDSE (*dashed red*), AHTMLE (*solid blue*) and OHTVT (*dashed black*)

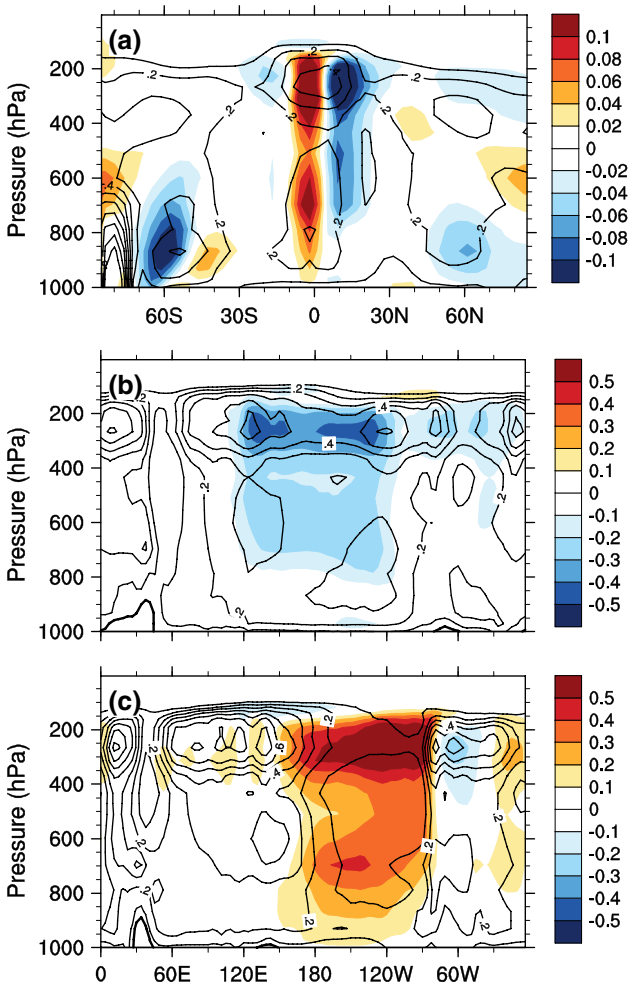

Fig. 14 Mean cloud (*contour*, CI = 0.1) in the CTRL and cloud changes (*color*) in 0.1 W run. **a** For the zonal averaged clouds, **b** for the clouds along 10°N and **c** for the clouds along 2°S

height over the 200 hPa is generally lowered in response to the overall cooling in the SST. In addition, Fig. 12b and d also illustrate a weakening in the zonal Walker Circulation, with a stronger anomalous convergence (divergence) over the eastern equatorial Pacific surface (200 hPa) in 0.1 W run, in accompany with the warming SST there and thus the enhanced HC.

5 Compensation and un-compensation

Several compensation changes are identified in this work. First of all, for the Earth's climate as a whole, the changes in the SW and LW at the TOA tend to be compensated. This compensation is nearly perfect in the mid-low latitudes within around 40°S–40°N (Fig. 4b), where the cloud plays a critical role (will be discussed later in Fig. 14). Second, the AHT and OHT in general have good compensation changes in the same latitudes, particularly in the deep tropics (Fig. 5b, d). Third, for the different components of OHT, the changes in the Eulerian mean and Bolus OHT are compensated with each other in the Southern Ocean (Fig. 13b), since stronger wind driven Ekman transport is associated with stronger meridional density gradient (stronger Bolus circulation) and vice versa. Fourth, for the different components of the AHT, the changes in the DSE and LE heat transports are compensated within the tropics (30°N/S), because stronger HC means the stronger equatorward convergence of the water vapour (Figs. 10f, 11c). Fifth, in the extratropics, the changes in the mean and eddy DSE transports show perfect compensation (Fig. 11f), as a result of the equatorward shift of the Ferrell Cell and enhancement of atmospheric baroclinicity in the mid-high latitudes, particularly over the North Atlantic. Sixth, the OHT change in

the NH extratropics appears to be partially compensated by the eddy AHT (Fig. 13c). This confirms the critical role of the atmospheric eddies (both stationary and transient) in maintaining energy balance in high latitudes. Nakamura et al. (1994) have proposed a positive feedback between the meridional atmospheric transport of moisture and the high latitude thermohaline circulation (the so-called EMT feedback), in which the partial compensation between the eddy AHT and the OHT is suggested. An increase in the northward fresh water transport reduces the high latitude sinking and thus the OHT, which in turn will increase the meridional temperature gradient and the baroclinic eddy transport. Seventh, this is the most important one, we have seen how the Earth's climate is trying to maintain the balance between two hemispheres (Fig. 13a): the ocean in the NH is colder than that in the SH due to the much reduced northward heat transport cross the Equator in the *Atlantic*, therefore, the atmosphere responds to the ocean with colder temperature in the SH than in the NH by transporting more heat northward cross the equator over the *Pacific,* as suggested by changes in the SST (Fig. 6a), the winds and pressure (Fig. 12b, d) as well as the net atmospheric heat flux (Figure not shown). We re-plotted Fig. 6a in Fig. 13a, in which the global mean SST and SAT are removed. So that the relative temperature change in the NH versus SH can be exhibited better. Figure 13a shows clearly the colder SST (SAT) in the NH (SH), as well as stronger meridional SST (SAT) gradient in the NH (SH).

The undercompensation (overcompensation) between the AHT and OHT changes is obvious in the extratropics (Fig. 5d). From the point of view of Earth's radiation energy balance (Fig. 4b), the outgoing LW heat flux in the NH high latitudes is weakened too much due to the dramatic temperature decrease, which cannot be compensated by the decrease in the downward SW, because here both the albedo and cloud change little. Although the sea ice increases its coverage toward the lower latitudes in the reduced wind run, the albedo in the high latitudes hardly changes. The cloud is also little altered (Fig. 14) because of few water vapour in the high latitudes. The sea ice albedo or the planetary albedo is one of the key factors in affecting the fundamental energy balance of the Earth (Stone 1978). Situation is different in the SH high latitudes. This occurs mainly in the ACC region, the area it is almost covered entirely by the sea ice in 0.1 W run, resulting in a much bigger decrease in the downward SW than that in the NH, because the sea surface area is much larger in the ACC than that in the North Atlantic. The Earth's energy re-balance shown in the Fig. 4 is the result, not the reason of the global MHT readjustment shown in Fig. 5.

From the point of view of dynamical change in the atmospheric and oceanic circulations, the undercompensation of the AHT to the OHT in the NH is due to big changes in the atmospheric Ferrell Cell (Fig. 10b, d, f). The heat transport by the Ferrell Cell tends to be out of phase with the eddy heat transport. This is true for both the mean state and their changes in the reduced wind run (Figs. 11d–f, 13c). The increase in the atmospheric eddy activities is offset by the change due to the Ferrell cell, resulting in an undercompensation of the AHT to the OHT decrease (Fig. 13c). In fact, the enhancement of the Ferrell Cell is connected to the equatorward shift of the ITCZ, that is, the HC. Therefore, the changes in the tropical atmosphere also play roles in the undercompensation of the AHT to the OHT in the NH mid-high latitudes. In the SH mid-high latitudes, however, the AHT change over-compensates the OHT change. This attributes to the big decreases in the Eulerian mean OHT as well as the bolus OHT in the ACC region. The atmosphere still feels the strong ocean surface cooling and responds with enhanced baroclinicity and thus stronger southward eddy AHT (Fig. 13c), which is not offset by the mean AHT change since the Ferrell Cell is roughly unchanged (Fig. 10f).

This paper focuses on the compensation. Since both the mean MHT and their changes in the high latitudes are small, the compensation issue itself over there is not that critical. We have seen that the MHT changes at the 40°N/S poleward are less than one-third of those in the tropics even in our extreme no-wind experiment. We have also seen the consistent pictures between the dynamical changes in the atmosphere and ocean circulations and the changes in the Earth's radiation budget in the un-compensation region. The less heat gain due to less poleward heat transport results in the less heat loss out of space. In the tropics, the good compensation should also be attributed to the clouds, which tends to affect the SW and LW oppositely, mitigating the poleward AHT change by enhancing the equatorward LE transport.

Finally the detailed cloud changes are examined in Fig. 14. The cloud amount increases over the equator and decreases along the 10°N (Fig. 14a), as a result of the southward shift of the ITCZ. Figure 14b further shows that it is the high cloud that decreases the most, which occurs mainly in the central-western Pacific of northern equator. The high cloud increase occurs mainly in the eastern Pacific to the south of equator (Fig. 14c). This is consistent with the weakening of the Walker circulation (Fig. 12). In the subtropics, the cloud change is trivial. In the high latitudes, the low cloud is generally reduced (Fig. 14a).

6 Conclusions and discussions

A coupled climate model is used in this work to study the wind effect on the MHT. Special interests are paid on the so-called BC between the changes in the OHT and AHT. The equilibrium responses are examined in this work. Figure 15 summarizes the main mechanisms that are involved

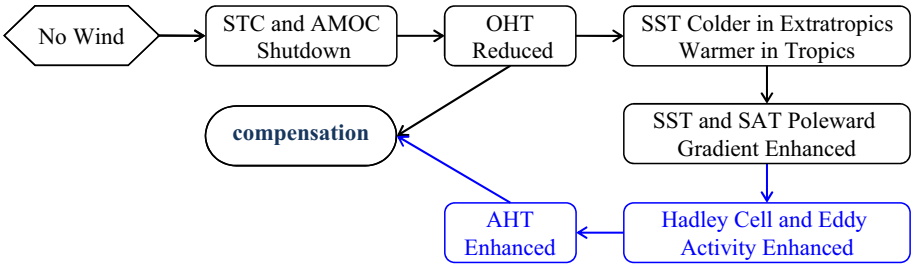

Fig. 15 Schematic diagram showing the main mechanisms that are responsible for the compensation between the changes in the AHT and OHT

in the compensation processes. The wind reduction can shut down both the STC and AMOC, resulting in decrease in the poleward OHT. The SST responds with significant warming in the equator and cooling off the equator, which feeds back to the atmosphere and causes an equatorward shift and enhancement in the HC. This in turn increases the poleward AHT, compensating the decrease of the poleward OHT. The total MHT of the global system remains nearly unchanged. This compensation suggests a fundamental constraint in the changes of ocean–atmosphere energy transport. In this work we also see the undercompensation (overcompensation) between the AHT and OHT changes in the extratropics. Since both the mean MHT and their changes in the mid-high latitudes are small, the compensation issue itself over there is not critical. The MHT changes at the 40°N/S poleward are less than one-third of those in the tropics even in our extreme no-wind experiment.

The opposite change in the atmospheric and oceanic meridional circulations is one of the key mechanisms to contain the Earth's climate variability. In this work the ocean meridional circulation changes, including both the STC and the AMOC, are mainly determined by the dynamical changes in the Ekman pumping, the Ekman advection as well as the sea ice advection in the mid-high latitudes. We also see that the salinity change determines the density change in the extratropics and eventually plays an important role in the AMOC change. This implies a critical role of hydrological cycle in the global energy adjustment. The ocean cooling in the high latitudes in response to the weakening of surface wind forcing tends to increase the density in the high latitudes. So the salinity decrease has to play a critical role in the AMOC weakening. Otherwise, the AMOC could be enhanced, and the changes in the AHT and OHT would be in phase instead of out of phase. There would be no so-called BC, and thus the global climate may drift dramatically due to lack of this restoring mechanism in the global energy adjustment. The salinity change in the high latitudes can be caused by the changes in the meridional salinity advection associated with the AMOC, the sea ice melting/formation, river runoff and the fresh water flux due to evaporation minus precipitation. The detailed mechanisms are examined in Yang et al. (2014b).

The good compensation between the AHT and OHT changes in the tropics should be also attributed largely to the good cloud feedback there. The big temperature change in the tropics causes dramatic change in the atmospheric convection and thus the clouds, which affects the SW and LW oppositely and tends to maintain the stability of the net radiation flux at the TOA. This ensures the perfect out of phase change in the AHT and OHT (Bjerknes 1964). Koll and Abbot (2013) have shown that the cloud feedback is critical for maintaining constant equatorial SST as OHT changes. We show in this work that the cloud feedback is critical for maintaining the constant net radiation flux at the TOA in the tropics, even with big SST change. In the mid-high latitudes, the cloud feedback is very weak so that the compensation in the OHT and AHT is imperfect. Cloud feedback is a critical stabilizing factor for the Earth's climate. We will further the study in our next work.

The atmospheric eddies play very important roles in energy balance in the mid-high latitudes. Without eddies' contributions, the energy deficit will be much severer. This also suggests a critical role of the atmospheric eddies in maintaining the high latitude Earth's climate stability, particularly the activities of eddies over the North Atlantic (Nakamura et al. 1994). By examining the changes in the atmospheric wind and pressure, we have found clues on the relative roles of the different ocean basins in the global atmospheric energy transport. The AHT change occurs mainly over the *tropical Pacific* and *extratropical Atlantic*, which are related to the mean circulation in the tropics and eddies' activities in the mid-high latitudes, respectively. In this work, the atmospheric eddies' contributions may be underestimated since the monthly data is used and the eddy AHT is obtained as the residual of the total AHT minus the mean AHT. This may also contribute to the un-compensation between the AHT and OHT changes. The role of eddies in global energy balance is worth investigating further.

This work focuses only on the equilibrium response in the global energy adjustment, providing the detailed analyses on 0.1 W run. The 0.3 and 0.5 W runs have the similar results that are not shown here for simplicity. Our next work is to explore the transient response of the AHT and OHT, in which we may disclose the interaction mechanism between the STC in the Pacific and the AMOC in

the Atlantic. Thus the roles of different ocean basins in the different stages of the climate change will be illuminated. Ensemble wind perturbation experiments focusing on the transient responses have been performed and the thorough analyses are underway.

Acknowledgments We are grateful to Profs. Z. Liu and R. Huang for invaluable suggestions and discussions. This work is jointly supported by the NSF of China (Nos. 91337106, 41376007, 41176002, 40976007), the National Basic Research Program of China (No. 2012CB955200), the Special Fund for Meteorological Scientific Research in the Public Interest of CMA (No. GYHY201006022) and the Norwegian Research Council through the East Asian DecCen project (No. 193690/S30). All the experiments are performed on the supercomputer at the LaCOAS, Peking University.

References

Bjerknes J (1964) Atlantic air–sea interaction. Adv Geophys 10:1–82

Carissimo BC, Oort AH, Vonder Haar TH (1985) Estimating the meridional energy transports in the atmosphere and ocean. J Phys Oceanogr 15:82–91

Chang P, Zhang R, Hazeleger W, Wen C, Wan X, Ji L, Haarsma RJ, Breugem WP, Seidel H (2008) Oceanic link between abrupt changes in the North Atlantic Ocean and the African monsoon. Nat Geosci 1:444–448

Cheng W, Bitz CM, Chiang JCH (2007) Adjustment of the global climate to an abrupt slowdown of the Atlantic meridional overturning circulation, ocean circulation: mechanisms and impacts. Geophys Monogr Ser 173:295–313

Czaja A, Marshall J (2006) The partitioning of poleward heat transport between the atmosphere and ocean. J Atmos Sci 63:1498–1511

Danabasoglu G, Marshall J (2007) Effects of vertical variations of thickness diffusivity in an ocean general circulation model. Ocean Model 18:122–141. doi:10.1016/j.ocemod.2007.03.006

Danabasoglu G, Bates S, Briegleb BP, Jayne SR, Jochum M, Large WG, Peacock S, Yeager SG (2012) The CCSM4 ocean component. J Clim 25:1361–1389. doi:10.1175/JCLI-D-11-00091.1

Drijfhout SS (2010) The atmospheric response to a thermohaline circulation collapse: scaling relations for the Hadley circulation and the nonlinear response in a coupled climate model. J Clim 23:757–774

Farneti R, Gent PR (2011) The effects of the eddy-induced advection coefficient in a coarse-resolution coupled climate model. Ocean Model 39:135–145. doi:10.1016/j.ocemod.2011.02.005

Farneti R, Vallis GK (2013) Meridional energy transport in the coupled atmosphere–ocean system: compensation and partitioning. J Clim 26:7151–7166. doi:10.1175/JCLI-D-12-00133.1

Fox-Kemper B, Ferrari R (2008) Parameterization of mixed layer eddies. Part II: prognosis and impact. J Phys Oceanogr 38:1166–1179

Fox-Kemper B, Ferrari R, Hallberg RW (2008) Parameterization of mixed layer eddies. Part I: theory and diagnosis. J Phys Oceanogr 38:1145–1165

Fox-Kemper B, Danabasoglu G, Ferrari R, Gries SM, Hallberg RW, Holland MM, Maltrud ME, Peacock S, Samuels BL (2011) Parameterization of mixed layer eddies. III: implementation and impact in global ocean climate simulations. Ocean Model 39:61–78

Gent P, McWilliams J (1990) Isopycnal mixing in ocean circulation models. J Phys Oceanogr 20:150–155

Held IM (2001) The partitioning of the poleward energy transport between the tropical ocean and atmosphere. J Atmos Sci 58:943–948

Huang R (2005) Contribution of oceanic circulation to the poleward heat flux. J Ocean Univ China 4:277–287

Hunke E, Lipscomb W (2008) CICE: The Los Alamos Sea Ice model, documentation and software user's manual, version 4.0. Tech Rep LA-CC-06-012, Los Alamos National Laboratory

IPCC Climate change (2007) The physical science basis summary for policymakers. Contribution of working group 1 to the fourth assessment report of the intergovernmental panel on climate change. Cambridge University Press, Cambridge

Koll DDB, Abbot DS (2013) Why tropical sea surface temperature is insensitive to ocean heat transport changes. J Clim 26:6742–6749. doi:10.1175/JCLI-D-13-00192.1

Laurian A, Drijfhout SS, Hazeleger W, van Dorland R (2009) Global surface cooling: the atmospheric fast feedback response to a collapse of the thermohaline circulation. Geophys Res Lett 36. doi:10.1029/2009GL040938

Lawrence DM, Oleson KW, Flanner MG, Fletcher CG, Lawrence PJ, Levis S, Swenson SC, Bonan GB (2012) The CCSM4 land simulation, 1850–2005: assessment of surface climate and new capabilities. J Clim 25:2240–2260. doi:10.1175/JCLI-D-11-00103.1

Long MC, Lindsay K, Peacock S, Moore JK, Doney SC (2013) Twentieth-century oceanic carbon uptake and storage in CESM1 (BGC). J Clim 26. doi:10.1175/JCLI-D-12-00184.1

Marshall J, Radko T (2003) Residual-mean solutions for the Antarctic circumpolar current and its associated overturning circulation. J Phys Oceanogr 33:2341–2354

Marshall J, Donohoe A, Ferreira D, McGee D (2013) The ocean's role in setting the mean position of the inter-tropical convergence zone. Clim Dyn. doi:10.1007/s00382-013-1767-z

Meehl GA, Washington WM, Arblaster JM, Hu A, Teng H, Kay JE, Gettelman A, Lawrence DM, Sanderson BM, Strand WG (2013) Climate change projections in CESM1 (CAM5) compared to CCSM4. J Clim. doi:10.1175/JCLI-D-12-00572.1

Nakamura M, Stone PH, Marotzke J (1994) Destabilization of the thermohaline circulation by atmospheric eddy transports. J Clim 7:1870–1882

Neale RB et al (2010) Description of the NCAR Community Atmosphere Model (CAM5.0), Tech Rep NCAR/TN-486+STR. National Center for Atmospheric Research, Boulder, CO, USA

Neale R, Richter J, Park S, Lauritzen P, Vavrus S, Rasch P, Zhang M (2013) The mean climate of the Community Atmosphere Model (CAM4) in forced SST and fully coupled experiments. J Clim 26:5150–5168. doi:10.1175/JCLI-D-12-00236.1

Philander SGH, Gu D, Halpern D, Lambert G, Lau N-C, Li T, Pancanowiski RC (1996) Why the ITCZ is mostly north of the equator. J Clim 9:2958–2972

Shaffrey L, Sutton R (2006) Bjerknes compensation and the decadal variability of the energy transports in a coupled climate model. J Clim 19:1167–1181

Smith RD et al (2010) The Parallel Ocean Program (POP) reference manual. Tech Rep LAUR-10-01853, Los Alamos National Laboratory

Stone PH (1978) Constraints on dynamical transports of energy on a spherical planet. Dyn Atmos Oceans 2:123–139

Swaluw EVD, Drijfhout SS, Hazeleger W (2007) Bjerknes compensation at high northern latitudes: the ocean forcing the atmosphere. J Clim 20:6023–6032

Timmermann A, Goosse H (2004) Is the wind stress forcing essential for the meridional overturning circulation? Geophys Res Lett 31:L04303. doi:10.1029/2003GL018777

Trenberth KE, Caron JM (2001) Estimates of meridional atmosphere and ocean heat transports. J Clim 14:3433–3443

Vallis GK, Farneti R (2009) Meridional energy transport in the coupled atmosphere–ocean system: scaling and numerical experiments. Q J R Meteorol Soc 135:1643–1660

Vellinga M, Wu P (2008) Relations between northward ocean and atmosphere energy transports in a coupled climate model. J Clim 21:561–575

Vonder Haar TH, Oort AH (1973) A new estimate of annual poleward energy transport by the oceans. J Phys Oceanogr 3:169–172

Wunsch C (2005) The total meridional heat flux and its oceanic and atmosphere partition. J Clim 18:4374–4380

Yang H, Wang L (2011) Tropical oceanic response to extratropical thermal forcing in a coupled climate model: a comparison between the Atlantic and Pacific oceans. J Clim 24:3850–3866

Yang H, Wang Y, Liu Z (2013) A modeling study of the Bjerknes compensation in the meridional heat transport in a freshening ocean. Tellus 65A. doi:10.3402/tellusa.v65i0.18480

Yang H, Li Q, Wang K, Sun Y, Sun D (2014a) Decomposing the meridional heat transport in the climate system. Clim Dyn. doi:10.1007/s00382-014-2380-5

Yang H, Wang K, Dai H, Wang Y, Li Q (2014b) Effects of wind and freshwater on the Atlantic meridional overturning circulation: role of sea ice and vertical mixing. Clim Dyn (submitted)

Zhang R, Delworth T (2005) Simulated tropical response to a substantial weakening of the Atlantic thermohaline circulation. J Clim 18:1853–1860

Zhang R, Kang SM, Held IM (2010) Sensitivity of climate change induced by the weakening of the Atlantic meridional overturning circulation to cloud feedback. J Clim 23. doi:10.1175/2009JCLI3118.1